Computational Methods

Computational models were developed using the commercial finite-element code ABAQUS (version 6.10, SIMULIA, Providence, RI). As discussed in the Results section, the iSPL is modeled as an initially flat rectangular plate composed of two layers (endoderm and splanchnic mesoderm). Appropriate symmetry conditions are enforced along the embryonic midline (Y-axis) throughout the simulation. Rollers are initially specified for the edges along the X and Y axes, with the other surfaces of the plate being free (Fig. 5). As described below, however, the boundary condition along the originally upper edge of the plate is changed during the simulation.

Hexagonal elements (C3D20R, 20-node) are used for both layers. The total model is discretized into 48256 elements. Testing with finer meshes (48256 elements, 4 elements across the thickness) confirmed that the chosen mesh size is accurate enough for the present purposes.

Basic Theory

Morphogenetic processes were simulated using a continuum mechanics theory for large deformation and growth of soft tissue (Rodriguez et al. 1994). Active contraction is modeled as negative growth along specified directions (Taber 2009). Here, we briefly describe the basic ideas.

The epithelia (mesoderm and endoderm) are assumed to respond approximately as pseudoelastic materials. The total deformation gradient tensor $\mathbf{F}$ is decomposed as

$$\mathbf{F} = \mathbf{F}^* \cdot \mathbf{G}, \tag{S1}$$

where $\mathbf{G}$ is the growth tensor and $\mathbf{F}^*$ is the elastic deformation gradient tensor. As the tissue grows, $\mathbf{G}$ changes the zero-stress configuration for each material particle, and $\mathbf{F}^*$ enforces compatibility between particles. Growth is included through the ABAQUS user subroutine UMAT, as described by Young et al. (2010).

In this theory, stress depends on the elastic part of the deformation. Because some water can enter or leave tissues as they deform, we treat epithelia as nearly incompressible with the Cauchy stress tensor $\boldsymbol{\sigma}$ given by the constitutive relation (Taber 2004)

$$\boldsymbol{\sigma} = \frac{1}{J^*}\mathbf{F}^* \cdot \frac{\partial W}{\partial \mathbf{E}^*} \cdot \mathbf{F}^{*T}. \tag{S2}$$

In this equation, $W(\mathbf{E}^*)$ is the strain-energy density function, $J^* = \det \mathbf{F}^*$ is the elastic volume ratio, and $\mathbf{E}^* = (\mathbf{F}^{*\mathsf{T}} \cdot \mathbf{F}^* - \mathbf{I})/2$ is the Lagrangian elastic strain tensor, with $\mathbf{I}$ being the identity tensor and T indicating the transpose.

Our earlier measurements for the blastoderm and heart tube in the early chick embryo suggest

that the material properties are relatively linear and isotropic (Varner & Taber 2012*a*, Zamir & Taber 2004, Varner et al. 2010). Accordingly, we take the strain-energy density function in the modified neo-Hookean form

$$W = C(\bar{I}_1 - 3) + \frac{1}{D}\left[\tfrac{1}{2}(J^{*2} - 1) - \ln J^*\right], \tag{S3}$$

where C and D are material constants, and $\bar{I}_1 = J^{*2/3}\,\mathrm{tr}\,\mathbf{C}^*$ is the modified first invariant of the elastic right Cauchy-Green deformation tensor $\mathbf{C}^* = \mathbf{I} + 2\mathbf{E}^*$. Having no data to the contrary, we assume that the mechanical properties for the mesoderm and endoderm are the same with $C = 10$ Pa and $D = 0.01$ Pa^{-1} for both layers (Shi et al. 2014).

For comparison to experimental measurements, the deformation-rate tensor was computed from the relation (Taber 2004)

$$\mathbf{D} = \mathbf{F}^{-T} \cdot \dot{\mathbf{E}} \cdot \mathbf{F}^{-1}, \tag{S4}$$

where $\mathbf{E}$ is based on the total deformation $\mathbf{F}$. The strain rate $\dot{\mathbf{E}}$ was calculated from the ABAQUS results using finite differences as described above for the experiments. The component of $\mathbf{D}$ tangent to the AIP is given by $D_T = \mathbf{n}_T \cdot \mathbf{D} \cdot \mathbf{n}_T$, where $\mathbf{n}_T$ is the unit vector tangent to the AIP in the deformed configuration.

Simulation procedure

As discussed above, the simulation consists of three phases (see Fig. 6). It is important to note that the growth tensor is defined relative to the initial geometry. Thus, $\mathbf{G}$ is specified in terms of material coordinates (X, Y, Z). The same set of axes is chosen for the spatial coordinates (x, y, z) in the current configuration.

Phase 1: Foregut formation. During Phase 1, differences in growth rate between the layers cause the iSPL to fold diagonally toward the midline of the embryo (Y-axis), creating the foregut pocket. The growth tensor is taken in the form

$$\mathbf{G} = G_X\,\mathbf{e}_X\mathbf{e}_X + G_Y\,\mathbf{e}_Y\mathbf{e}_Y + G_Z\,\mathbf{e}_Z\mathbf{e}_Z \tag{S5}$$

for both layers with $\mathbf{e}_i$ being Cartesian unit base vectors. Accordingly, $G_i = 1$ for no growth, $G_i > 1$ for positive growth, and $G_i < 1$ for negative growth or active contraction. Experiments have revealed that the cell proliferation rate in the folding endoderm of HH6–8 chick embryos increases in the cranial and medial directions (Bellairs 1955, Miller et al. 1999). Assuming that

Development • Supplementary information

this trend also holds for the mesoderm, we stipulate the growth rates

$$\begin{aligned}\dot{G}_X(X,Y) &= \alpha_X(1-\bar{X})\bar{Y}\\ \dot{G}_Y(X,Y) &= \alpha_Y(1-\bar{X})\bar{Y}\Delta(X)\\ \dot{G}_Z &= 0\end{aligned} \tag{S6}$$

during Phase 1, where α_X and α_Y are constants, dot denotes time differentiation, and

$$\bar{X} = X/a, \qquad \bar{Y} = Y/b, \tag{S7}$$

in which a and b are dimensions of the plate (Fig. 5A). The equations are integrated with $G_X = G_Y = G_Z = 1$ everywhere at $t = 0$. Note that we assume growth increases linearly with time.

To give reasonable agreement with observed changes in morphology, a parameter study (Fig. S3) provided the values $(\alpha_X, \alpha_Y) = (0.35, 0.9)$ h^{-1} in the endoderm and $(0.7, 1.0)$ h^{-1} in the mesoderm during Phase 1. Over a period of three hours, the values for the endoderm yield average growth $G_x \approx 1.5$ and $G_y \approx 3.2$ in the iSPL, compared to experimental values of 1.6 and 2.1, respectively (see Fig. 4C). The normalized distribution for $\dot{G} = \dot{G}_X/\alpha_X = \dot{G}_Y/(\alpha_Y\Delta)$ during Phase 1 is shown in Fig. 5D.

Note that Eq. (S6)$_2$ contains the function $\Delta(X)$. Initially, we set $\Delta = 1$, but as the iSPL folds and the originally upper edge of the iSPL approaches the embryonic midline, Δ becomes the distance from the Y-axis for each point along the this edge, i.e., $\Delta = x(X, b, 0)$. Thus, $\dot{G}_Y \to 0$ as $\Delta \to 0$, preventing the edge from passing the midline, where it would contact the opposite iSPL in a full model including both sides of the embryo. In this sense, including Δ provides an additional symmetry condition.

At the end of Phase 1, the upper edge of the iSPL is aligned with the embryonic midline (Y-axis; see Fig. 6, first row, HH7). Before Phase 2 begins, we simulate fusion of the iSPL with its mirror image on the other side of the embryo by changing the boundary conditions along this edge from free to symmetry conditions. In addition, subsequent motion of the edge originally along the Y-axis is prevented by changing the boundary conditions from roller to fixed to simulate attachment of the midline to the relatively stiff notochord (Koehl et al. 2000).

Phase 2: AIP descension During Phase 2 (HH7–HH9; $t = 4$–10 h), contraction tangential to the AIP is simulated by specifying negative growth in the Y direction within the relatively thin region of endoderm representing the AIP region (green, Fig. 5C). In this region, therefore, we set $\dot{G}_Y = -0.3$ h^{-1} and $\dot{G}_X = \dot{G}_Z = 0$. Also, because contracting tissues stiffen, the modulus C increases from 10 to 100 Pa as it shortens (Varner & Taber 2012*a*).

Contraction along the arch-shaped AIP pulls the lower edge of the iSPL downward, stretching

Development • Supplementary information

the iSPL axially and lengthening the FG and heart-forming regions (Fig. 6, top row, Phase 2). To partially relax the tension increase above the AIP, we include growth in this region in the y direction, i.e., the original X direction, consistent with experiments suggesting that cell proliferation occurs in the floor (ventral side) of the foregut as the AIP descends (Kirby et al. 2003). Thus, we set $\dot{G}_X = 0.2$ h^{-1} and $\dot{G}_Y = \dot{G}_Z = 0$ in both layers outside the AIP during Phase 2.

Phase 3: Heart tube formation During Phase 3 (HH9–HH10; $t = 10$–15 h), the growth rate increases in the heart-forming region, causing it to bulge away from the endoderm to create the HT. During this phase, cardiac jelly pressure p between the endoderm and HF is specified, with p increasing linearly in time from zero to 2 Pa, a value somewhat less than published measurements in the HH12 chick heart (Manasek et al. 1984). Within the HF region of the mesoderm, growth is specified to occur in the deformed circumferential and radial directions at the rates $(\dot{G}_Y, \dot{G}_Z) = (0.25, 0.3)$ h^{-1}. Growth is turned off elsewhere.

In the embryo, the oSPL affects the shape of the HT as it expands (see Fig. 6, bottom row, HH10). This effect is simulated by adding a flat plate positioned ventrally to the growing HT (Fig. 6, middle row, HH10). As the HF grows and contacts the plate, frictionless contact is enforced.

Experimental Methods

Visualization of Cell Proliferation. To visualize proliferation in control and aphidicolin-treated embryos, the Click-iT EdU (5-ethynyl-2'-deoxyuridine) assay (Invitrogen) was used to label cells undergoing DNA synthesis. To optimize EdU incorporation in chick embryos, EdU was diluted to 1 mM in phosphate-buffered saline (PBS), and 400 μL of EdU solution was pipetted directly on top of HH5 embryos as described by Warren et al. (2009). Embryos were incubated with EdU for four hours (to approximately HH7), then immediately fixed in 3.7% formaldehyde. Whole embryos were permeabilized for one hour in 1% bovine serum albumin (Sigma) and 0.1% Triton X-100 (Sigma) (Filas et al. 2012) before applying the Click-iT EdU reaction cocktail according to the manufacturer protocol. To stain DNA in both labeled and unlabeled cells, samples were also incubated in 5μg/mL Hoechst 33342 for 30 minutes according to the Click-iT EdU protocol.

After staining, whole embryos were imaged using a Zeiss LSM 710 confocal microscope. Three-dimensional image stacks were recorded at 20x magnification with z-spacing (ventral to dorsal) of 2 μm between each slice. Image stacks were rotated and converted to maximum-intensity z-projections using ImageJ.

Development • Supplementary information

Measurement of Tissue Deformation and Growth. Deformation was quantified from the motions of microbeads injected into the tissue. To compute deformation rate, ImageJ was used to measure the arc length $L(t_i)$ at each time point t_i along the AIP between pairs of neighboring beads lying within the same focal plane (Fig. 9A,B). The deformation rate tangential to the AIP was then computed as

$$D_T(t_i) = \frac{L(t_i) - L(t_{i-1})}{L(t_i)\Delta t},$$

where $\Delta t = t_i - t_{i-1}$. At the initial time, the corresponding forward difference was used to compute D_T. Results were then pooled to compute the average value of D_T along the AIP (arrows in Fig. 9A) at each t_i.

To compute growth, we assumed that the deformation is dominated by normal strains in the x and y directions. Then, Eq. (S1) gives the total stretch ratios

$$\lambda_x = \lambda_x^* G_x, \qquad \lambda_y = \lambda_y^* G_y, \tag{S8}$$

where the λ_i^* and G_i are components of $\mathbf{F}^*$ and $\mathbf{G}$, respectively. Lagrangian strains E_{xx} and E_{yy} were computed from the coordinates of triangular arrays of beads as described in Taber et al. (1994), and then $\lambda_x = \sqrt{1 + 2E_{xx}}$ and $\lambda_y = \sqrt{1 + 2E_y}$ were calculated. The elastic stretch ratios λ_i^* were found from hole-punching experiments (see Materials and Methods in the main text). Then, Eqs. (S8) provided G_x and G_y.

Development • Supplementary information

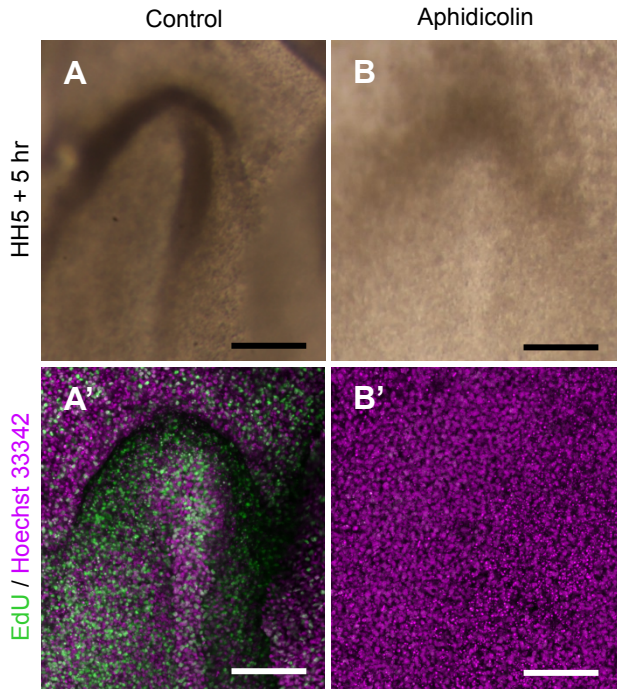

Figure S1: **Aphidicolin inhibits proliferation in the splanchnopleure (SPL).** Control and aphidicolin-treated embryos were labeled with EdU during Phase 1 development ($n = 4$ and $n = 3$, respectively). (A, B) Brightfield images of embryos after culture to HH7. (A', B') Confocal images of same embryos labeled with EdU (green) to show nuclei undergoing DNA synthesis and Hoechst 33342 (magenta) to show all nuclei, including those not undergoing DNA synthesis. EdU-labeled nuclei confirm DNA synthesis throughout the SPL of control embryos. EdU incorporation was greatly reduced in aphidicolin-treated embryos, suggesting that proliferation has been inhibited. Scale bars are 300 μm.

Development • Supplementary information

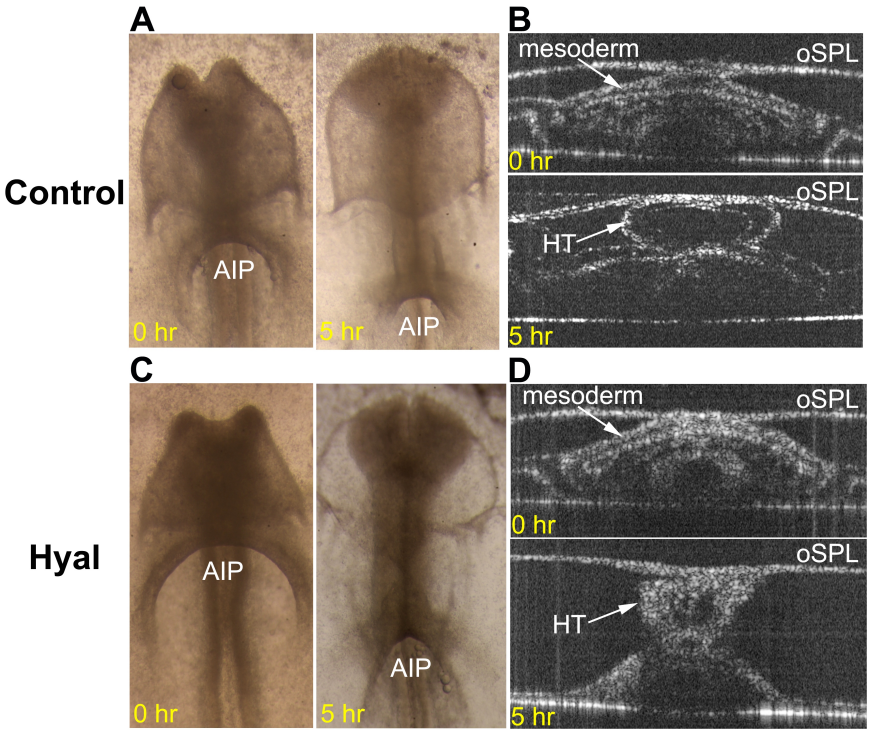

Figure S2: **Effects of removing cardiac jelly. (A, C)** Representative chick embryos cultured for 5 h from stage HH8 in normal media and in media containing 20 UTR/mL hyaluronidase (Hyal) (ventral view). Yellow dashed lines indicate anterior intestinal portal (AIP). Scale bar = 175 μm. **(B, D)** OCT images of transverse cross-sections indicated by dashed white lines in A and C, respectively. Scale bar = 50 μm. The heart tube (HT) formed in both cases, but it was considerably smaller in embryos exposed to Hyal. EN = endocardium; oSPL = outer splanchnopleure

Development • Supplementary information

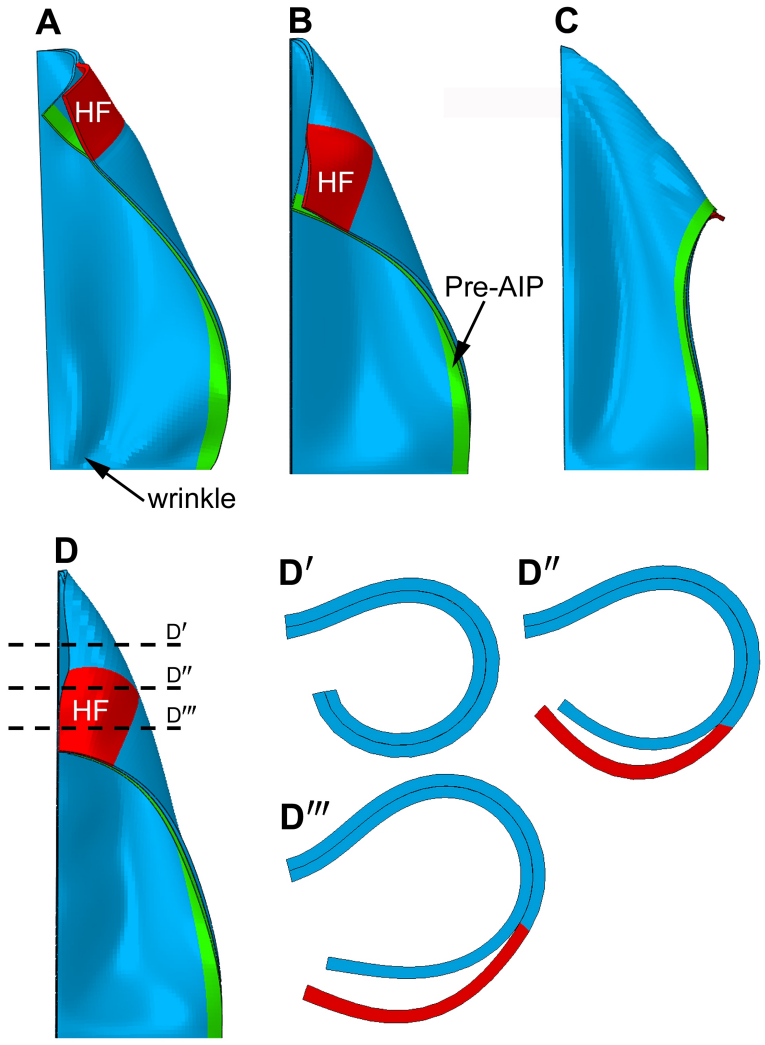

Figure S3: **Parameter study: effects of changing growth patterns. (A)** No growth gradient. The upper edge of the iSPL rotates an insufficient amount to align with the embryonic midline. **(B)** Growth rates (α_X and α_Y) in mesoderm are doubled. The caudal edge of the iSPL meets the midline before the cranial edge, contrary to observations. **(C)** Growth rate α_Y in mesoderm is decreased by 50%. Dorsal folding occurs. **(D–D‴)** Growth rate α_Y in mesoderm is increased by 50%. Ventral and cross-sectional views show that the membrane curls too much before reaching the midline. HF = heart field; AIP = anterior intestinal portal.

Development • Supplementary information

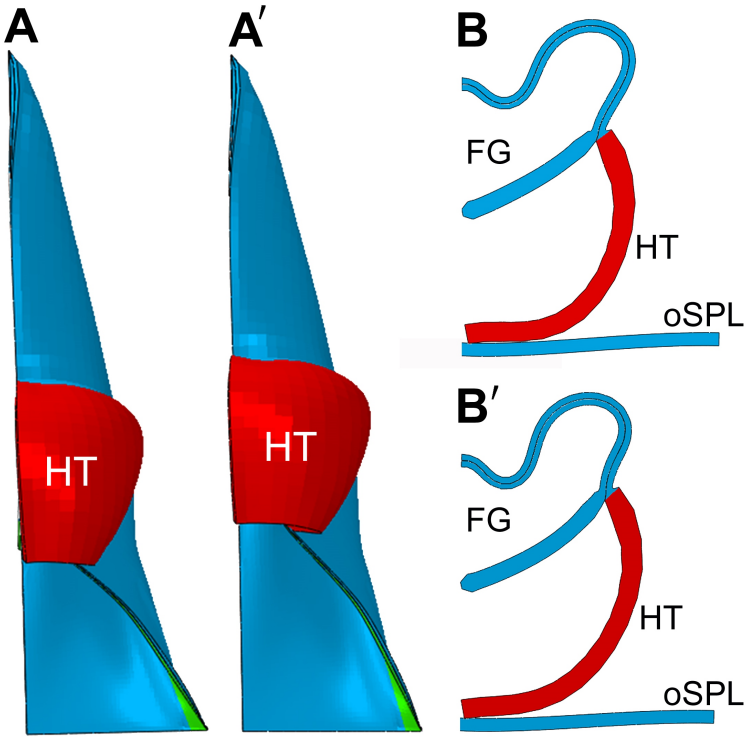

Figure S4: **Parameter study: effects of AIP stiffness and cardiac jelly pressure. (A)** Normal model with AIP border (green) stiffening as it contracts. **(A′)** Same model without increase in AIP stiffness. AIP descends a lesser amount. **(B)** Normal model cross section at HH10. **(B′)** Same model without cardiac jelly pressure. Shape of cross section changes only slightly. HT = heart tube; FG = foregut; oSPL = outer splanchnopleure

Development • Supplementary information

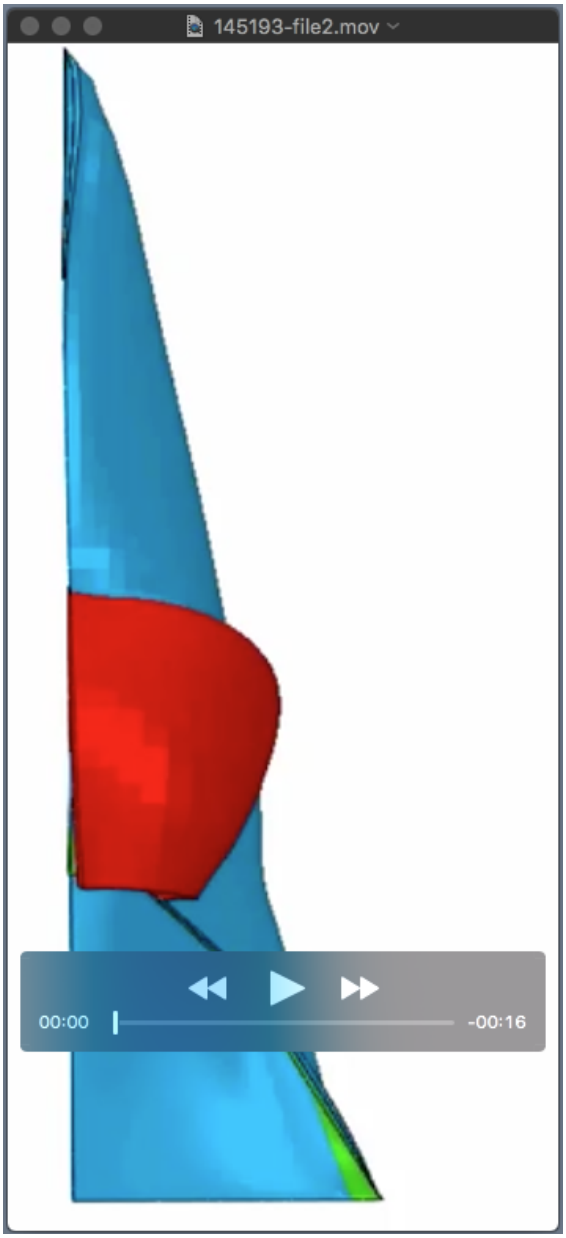

Movie 1: Ventral view of computational model.

Development • Supplementary information

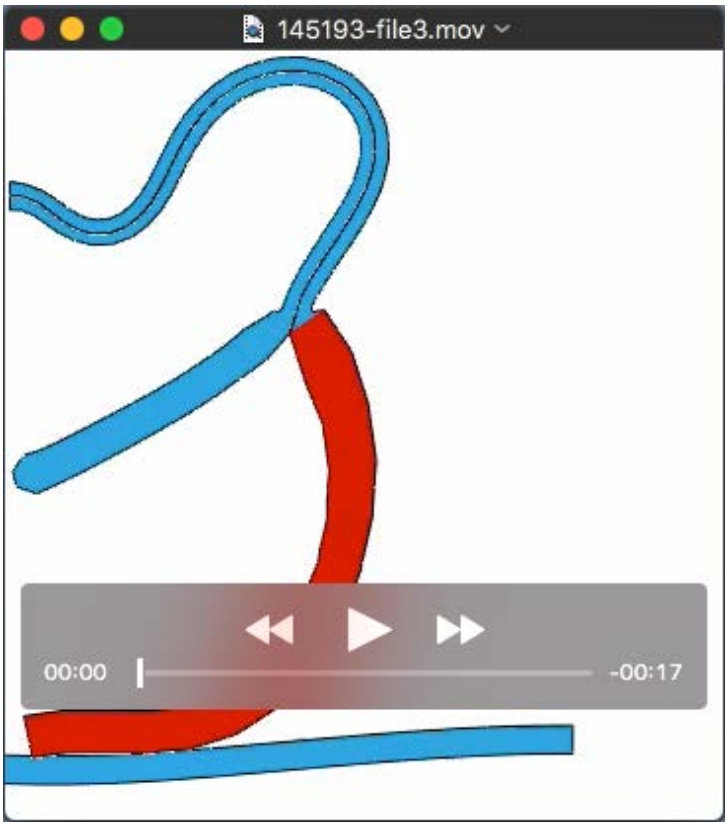

Movie 2: Cross-sectional view of computational model.

Development • Supplementary information